Int J Adv Manuf Technol (2008) 39:512–520
DOI 10.1007/s00170-007-1240-4

ORIGINAL ARTICLE

Modeling and simulation of non-uniformity in the planarization process

Thin-Lin Horng

Received: 12 June 2007 / Accepted: 11 September 2007 / Published online: 5 October 2007

Abstract The estimation of surface non-uniformity under various machining parameters (such as dressing force, diamond density of dresser, rotational speed of dresser, different machining paths, etc.) is essential to the planarization process. Based on abrasive theory and the deformation analyses of a polishing pad, this paper develops a model to calculate material removal in the planarization process and then calculate non-uniformity by using this model. The results reveal that the non-uniformity is in good agreement with experimental data. Moreover, it was found that the non-uniformity decreased when the dressing time increased.

Keywords Non-uniformity · Material removal · Deformation · Planarization

1 Introduction

One of the most important factors to be concerned within CMP is the polishing pad. The polishing pad needs to be dressed to maintain the quality and the throughput of production due to the wear of the pad and the influence of impurities. In the pad dressing process, the magnitude of non-uniformity plays a pivotal role in the time needed, the abrasive efficiency, and the wear of abrasive particles [1].

Preston [2] presented an empirical method to estimate glass materials by using an equation related to the pressure and relative speed, and a number of studies [3] have been carried out to modify this equation. Tseng [4] conducted a study to elucidate the roles of common mechanical characteristics in the removal process. In the study, he found that the particle removal rate could be remarkably enhanced by increasing pressure (dressing force), while increasing the pad rotation speed (shear stress) contributes little to increase the particle count. Xie [5] presented the mechanisms of material removal in the free-abrasive polishing process and recommended that when polishing a pad, in order to achieve a high materials removal rate and a smooth surface, it is preferable to use diamond as the polishing material because of its high deformation resistance. Goryacheva [6] examined wear rate by performing an experiment for typical dependence of linear wear on testing time. In the dressing process, she found that the polishing pad deformed severely when a high wear rate was achieved. Lin [1] conducted an experiment to reveal the effects of polishing parameters, such as rotational speed, applied pressure, locations of nozzles for slurry, and flow rate on surface characteristics when polishing an aluminum-based rigid disk. Horng [7] demonstrated a deformation equation to find the pad deformation during dressing, and also suggested that investigating pad deformation is essential to calculate the wear rate accurately. Thomas [8] explored Cartesian coordinate maps to calculate non-uniformity for chemical mechanical planarization. However, the estimation of non-uniformity by using pad deformation appears to be neglected in previous research work. Venkatesh [9] performed research on the polishing of glass mold that were first milled and then lapped with hard and soft pellets in the optical industry and found the familiar knee curve, after which an increase in polishing time does not improve the surface finish.

Based on abrasive theory [5] and the deformation analyses of a polished pad in the planarization process [7], this paper proposes a model to estimate non-uniformity. Moreover, simulation of the process was conducted under

T.-L. Horng (✉)
Department of Mechanical Engineering, Kun-Shan University, Tainan, Taiwan, Republic of China
e-mail: hortl@mail.ksu.edu.tw

various machining parameters, such as abrasive force, rotational speed of dresser and various machining paths. The abrasive depth was obtained by adding the abrasive quantities of every abrasive particle attached to the dresser and the non-uniformity can be obtained by statistical methods. Compared to the typical dependence of linear wear on testing time done by Goryacheva [6], and polishing time versus surface roughness curves conducted by Venkatesh [9], the model demonstrated in this paper can be a good simulation of non-uniformity for pad dressing in the planarization process.

2 Modeling the planarization process

2.1 Configuration of dresser and abrasive particles

The pad dressing process shown in Fig. 1 was simulated by the abrasive effect between pad and diamond particles bound to the dresser. The configuration of dressers shown in Fig. 2 is symmetrical to the center of the holder, and dressing forces were applied to the dresser equally. If the contact surface between the dresser and polishing pad is assumed to be a flat plane, then the dressing model can be simplified as the plate is subjected to a multi-uniformly circular load.

In the dressing process, the abrasive particles of diamond grain with a nearly round shape [5], referred to as R-type, are always suggested. In this study, the R-type diamond dresser [10], shown in Fig. 3 and Fig. 4, was used and the diamond grain was simulated as a half sphere. Moreover, a rectangle-type configuration with constant distance between diamond grains, shown in Fig. 5, was used to simulate the distribution of diamond particles on the dresser.

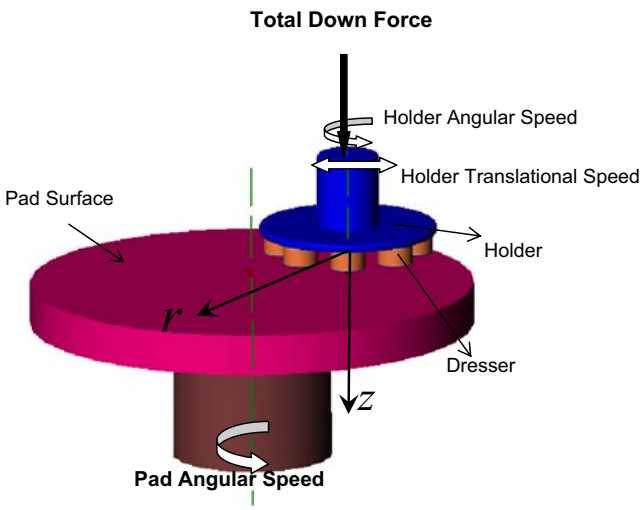

Fig. 1 Pad dressing process

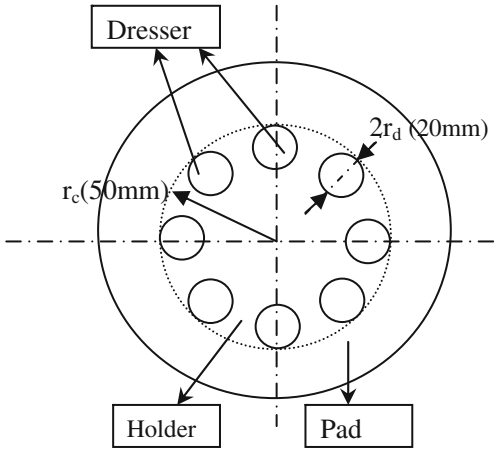

Fig. 2 Configuration of the dresser and polishing pad

2.2 Modified rotary dressing path

The modified rotary dressing path [10], shown in Fig. 6, was used to investigate the planarization process for the pad. In the dressing process, the holder and polishing pad revolve on their own axis with angular speeds, ω_d and ω_p, respectively. Simultaneously, the holder translates to and fro on the pad surface with a constant speed V_d. The locus of diamond particle P attached to the dresser can be described by *x(t) y(t)* as:

$$x(t) = \overline{OP}\cos\left(\omega_P \times t + \Psi_0\right) + V_d \times t \tag{1}$$

$$y(t) = \overline{OP}\sin\left(\omega_P \times t + \Psi_0\right) \tag{2}$$

$$\overline{OP} = \sqrt{\begin{aligned}&\left[e + (r_c - r_d)\cos\omega_d t + \overline{O_2P} \times \cos\theta\right]^2 \\ &+\left[(r_c - r_d)\sin\omega_d t + \overline{O_2P} \times \sin\theta\right]^2\end{aligned}} \tag{3}$$

$$\Psi_0 = Tan^{-1}\left(\frac{(r_c - r_d)\sin\omega_d t + \overline{O_2P} \times \sin\theta}{e + (r_c - r_d)\cos\omega_d t + \overline{O_2P} \times \cos\theta}\right) \tag{4}$$

where

$\overline{OP}$	The radial distance of the particle considered about center of pad
Ψ_0	The angle between $\overline{OP}$ and x-axis
$\overline{O_2P}$	The radial distance of the particle considered about center of dresser
θ	The angle between $\overline{O_2P}$ and x-axis
ω_d	Angular speed of the holder, V_d: translation speed of the holder, ω_p : angular speed of the pad.
r_c	Radius of the holder, r_d : radius of the dresser, e : eccentric length.

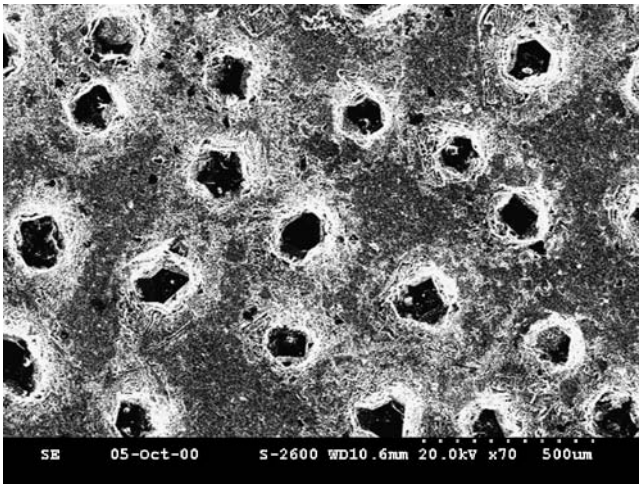

Fig. 3 R-type diamond dresser 10

3 Non-uniformity estimation for pad dressing in the planarization process

3.1 Deformation of a polishing pad subjected to a multi-dresser

Based on the results of Horng [7], the deformation of a point along the line y=0, due to the load on a line parallel to the x-axis with a length of $2\sqrt{r_d^2-\xi^2}$ and a width of $d\xi$, can be written as:

$$\varpi(r,0,z)=\frac{(1+\nu)}{2\pi E}\left\{\frac{2\left[r_d^2-\xi^2\right]^{1/2}z^2}{\left[(r-\xi)^2+z^2\right]\left[(r-\xi)^2+r_c^2-\xi^2+z^2\right]^{1/2}}\right\}p(\xi)d\xi + \frac{(1+\nu)}{2\pi E}\left\{4(1-\nu)\ln\left(\frac{\left[r_d^2-\xi^2\right]^{1/2}+\left[(r-\xi)^2+r_d^2-\xi^2+z^2\right]^{1/2}}{\left[(r-\xi)^2+z^2\right]^{1/2}}\right)\right\}p(\xi)d\xi. \quad (5)$$

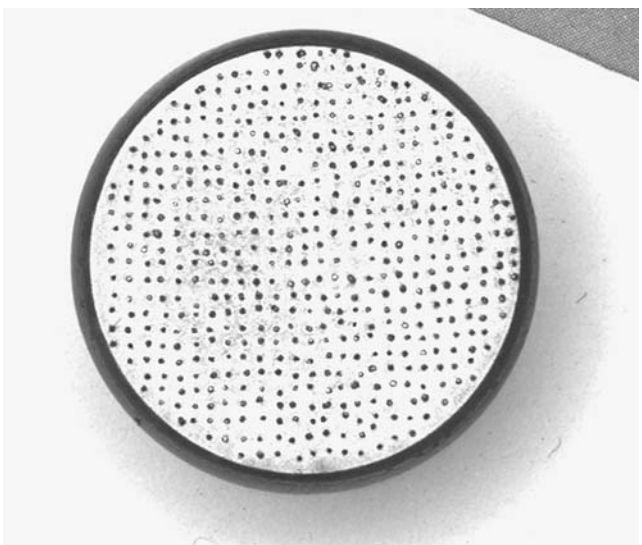

Fig. 4 Configuration of the diamond grain on the dresser 10

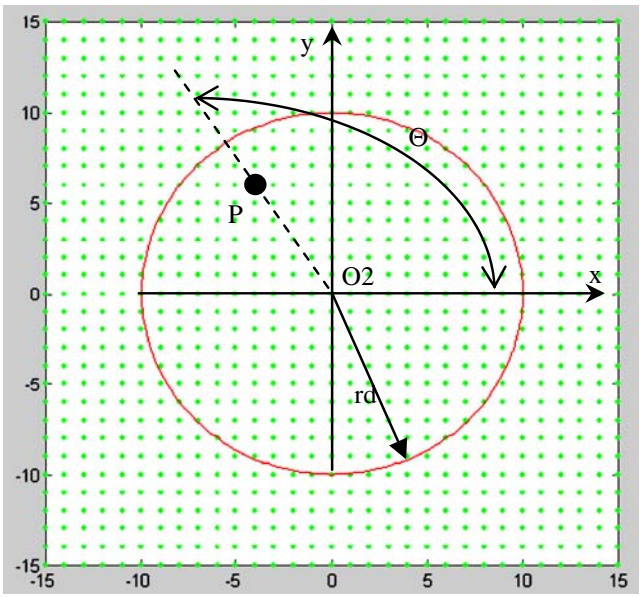

Fig. 5 Abrasive particles with constant distance

where z is absolute deformation and r is the coordinates shown in Fig. 1, v is the Poisson's ratio, E is the Young's modulus of the plate and $p(\xi)$ is the contact pressure applied on the pad.

The effect of pad thickness on deformation can be taken into account in the manner used by Dowson and Higginson [11] by setting r=0 and z=H, where H is the thickness of the pad. The pad deformation along the radial direction is calculated relative to this reference point (r=0, z=H) in the half space. Thus, the relative displacement between (r, 0, 0) and (0, 0, H), due to the uniform load from $\xi=-r_d$ to $\xi=r_d$, becomes:

$$u(r)=\int_{-r_d}^{r_d}(\varpi(r,0,0)-\varpi(0,0,H))d\xi \quad (6)$$

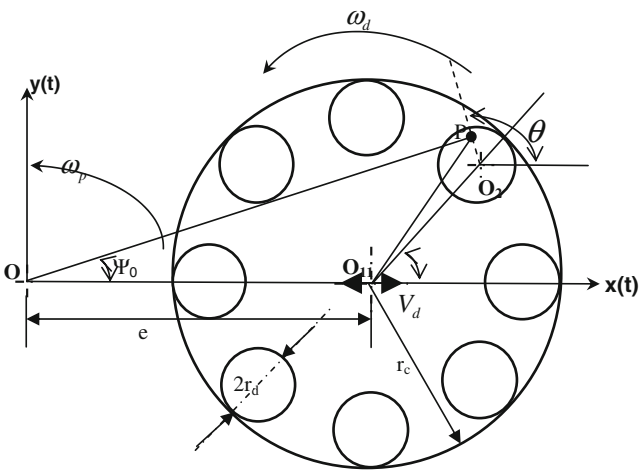

Fig. 6 Modified rotary dressing path

where r_d is the radius of the dresser and H is the thickness of the pad. For a uniform load distribution

$$p(\xi) = \frac{P}{\pi r_d^2}. \tag{7}$$

where P is the dressing force.

Deformation of a pad subjected to a single dresser can be calculated by using Eq. 6. The superposition method is introduced to calculate the deformation caused by the N_d dresser. Thus, deformation of a polishing pad at time t can be expressed as

$$\delta(t) = \sum_{i=1}^{N_d} \left\{ \int_{-r_d}^{r_d} \left[\varpi\left(\sqrt{x^2(t) + y^2(t)}, 0, 0 \right) - \varpi(0,0,H) \right] d\xi \right\} \tag{8}$$

where N_d is the number of dressers.

3.2 Material removal model

The R-type diamond grain was simulated in this study. The grain was modeled as a half sphere subjected to the dressing force, as shown in Fig. 7. In the dressing process, the grain will slide on the pad surface with the dressing speed, and undergo a sliding distance L from time t_1 to t_2 on the pad surface and the relative deformation of the polishing pad for the time interval, denoted as $(t_1–t_2)$, which can be expressed as

$$\Delta(t) = \delta(t_2) - \delta(t_1) \tag{9}$$

and can be obtained by Eq. 9.

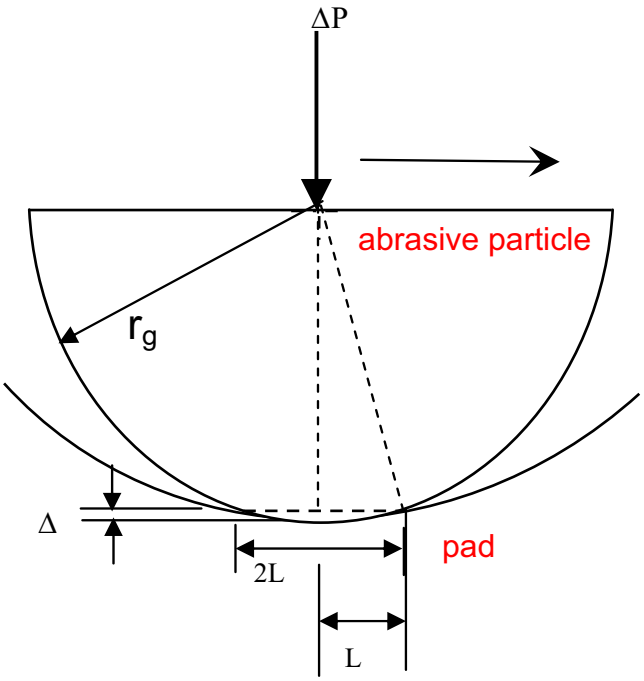

Fig. 7 Interfaces between pad and an abrasive particle

When the applied load ΔP is acting on a grain particle, the contact between the diamond and the pad is either plastic or elastic. During plastic contact, $\Delta P = H_p S_p$, where H_p and S_p are the hardness and the plastically deformed surface area of the diamond grain and pad, respectively. For a spherical particle with radius r_g, $S_p = 2\pi r_g \Delta$, where Δ is the relative deformation of the pad (see Fig. 3). When Δ is small enough, the contact between the diamond grain and the polished surface is elastic. In such cases, the wear rate will be negligible. When $\overline{p} = \Delta P / (2\pi r_g \Delta) \geq H_p$, where $\overline{p}$ is the mean contact pressure between the grain particle and the polished pad surface, the contact surface becomes plastic and the wear effect occurs.

If the material removal rate is defined as the volume of removed material from the surface V, divided by the sliding distance L, i.e., $K = V/L$, the contribution that a particle which is in plastic contact with the polished surface makes to the wear coefficient is $dK = dV/L = c \times ds \times L/L = c \times ds$, where c is a fraction of the displaced material which becomes loose debris and is a constant related to the material property and ds is the cross-section area of the worn groove caused by the particle. In practice, Δ is very small compared with the particle r_g, so $ds \approx L\Delta$ and $\Delta/L \approx L/r_g$. Then, $L \approx \sqrt{r_g \Delta}$ is obtained and the material removal conducted by one abrasive particle can be written as:

$$dv_i(t) = c\sqrt{r_g \Delta^3(t)} \times L. \tag{10}$$

Finally, the material removal rate V, which is function of time t, can be obtained by

$$V(t) = \sum_{i=1}^{N} dv_i(t) \tag{11}$$

where N is the number of abrasive particles.

3.3 Validation of the material removal model

In order to verify the material removal model, a dressing process with a modified rotary dressing path was modeled to investigate the material removal, and the simulation results were compared to the experimental results conducted by Goryacheva [6]. Fig. 6 shows this model and its dimensions, where E (elastic modulus)=139.47 Mpa, ν (Poisson's ratio)=0.3, f_c (Dressing force)=130 N, d_n (Density of the diamond grain on dresser)=200 No./cm^2, ω_d (Angular speed of the holder)=30 rpm, ω_p (Angular speed of the pad)=20 rpm, V_d (Translation speed of the pad)=3 mm/s, r_g (Average radius of diamond grain)=0.01 mm, N_d (Number of dressers)=8, r_d (Radius of dresser)=10 mm, r_c (Radius of dresser holder)=50 mm, r_p (Radius of pad)=400 mm, H (Depth of pad)=4 mm, e (Eccentric length)=200 mm and c (A fraction of displaced material)=0.5.

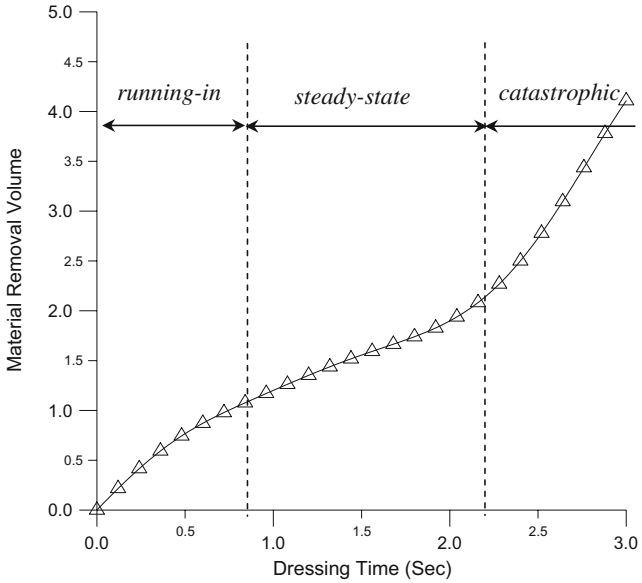

Fig. 8 Typical material removal volume V histories unit of V: $\mu^3/1000$

At the beginning of the wear process, called the running-in period, the material removal shown in Fig. 9 is increasing more rapidly than that in Fig. 8. This is because the self-organizing processes of the system hold in the typical dependence of linear wear experiment, as shown in Fig. 9 [6]. The running-in period gives way to the steady-state stage of wear, for this time period ($t_1<t<t_2$), the material removal is directly proportional to the testing time or the sliding distance, i.e., the wear rate (intensity) does not change. In this stage, material removal shown in Fig. 9 is similar to that in Fig. 8. The reason is that at this stage of the process, the wear characteristics which appear in the wear equation are registered. The results are also valid

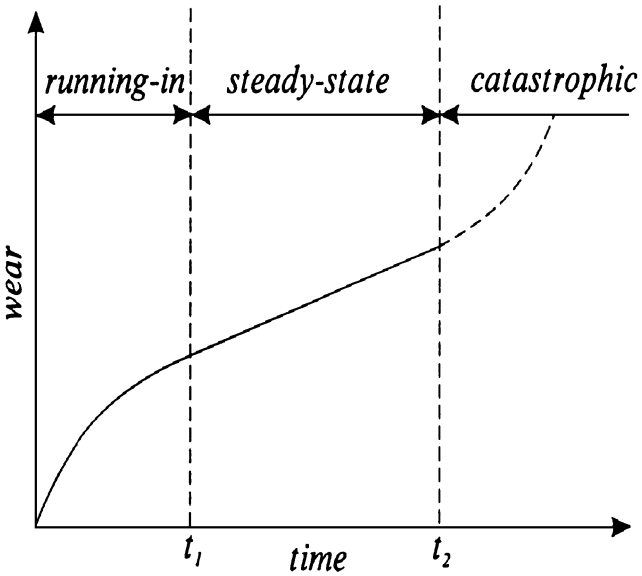

Fig. 9 Typical dependence of linear wear on testing time (Goryacheva [6], Fig. 6.1, pp. 193)

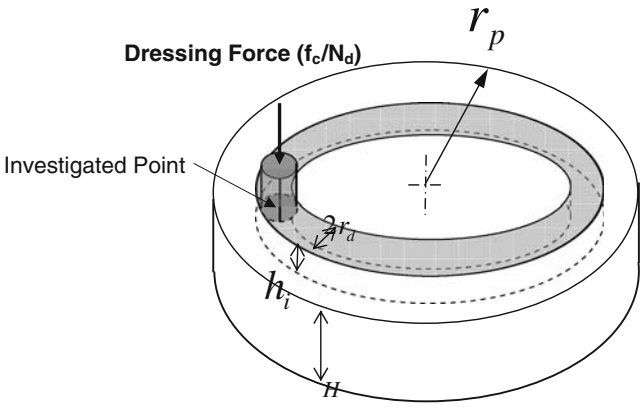

Fig. 10 Configuration of abrasive depth to calculate non-uniformity

when a stage of catastrophic wear ($t>t_2$) approaches, especially for inhomogeneous materials and for modified surfaces. From the previous comparison between Fig. 8 and Fig. 9, the model presented in this paper can be an acceptable estimation for wear rate calculation in the pad dressing process.

3.4 Non-uniformity Estimation

By using the material removal model mentioned before and assuming that the volume of material removal conducted by the single dresser is uniform, the abrasive depth h_i at the investigated point i on the pad surface, shown in Fig. 10, can be expressed as:

$$h_i(t) = \frac{V(t)}{\pi r_d^2} \tag{12}$$

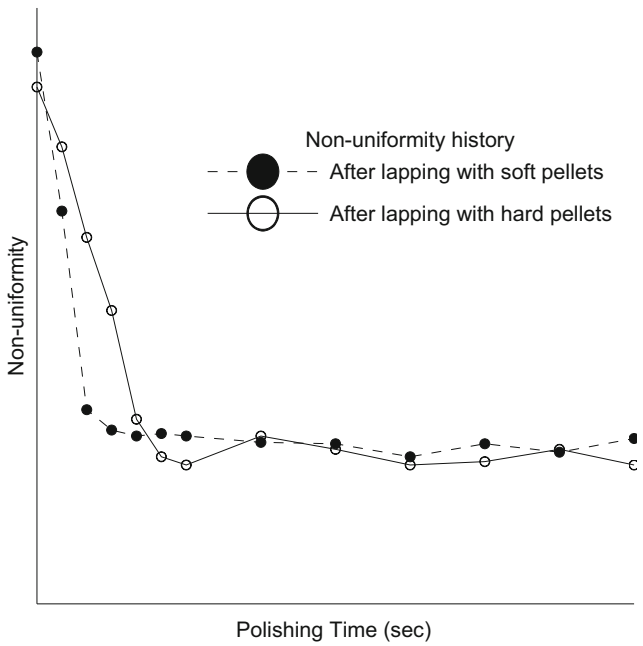

Fig. 11 Experimental data on non-uniformity collected by Venkatesh [9]

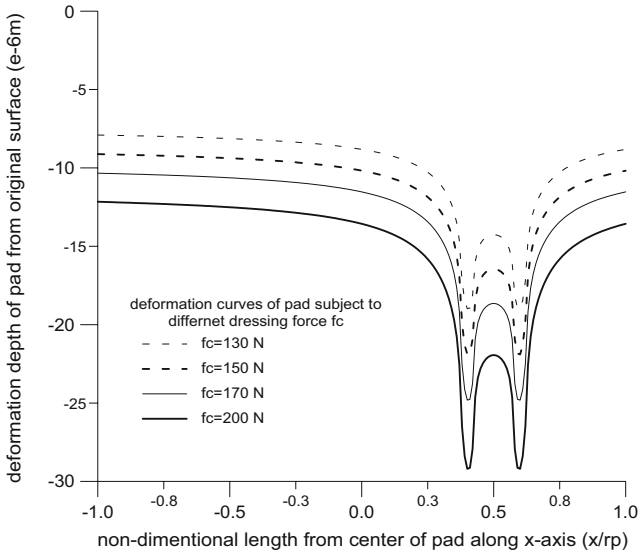

Fig. 12 Typical deform curves along the x- direction of pad

Then, the mean abrasive depth of the surface of pad, denoted by $\overline{h}$, can be written as:

$$\overline{h}(t) = \sum_{i=1}^{N_c} h_i(t) \Big/ N_c \tag{13}$$

where *Nc* is the number of investigated points on the pad. Finally, the square mean method is introduced to describe the non-uniformity. Index *Nu*, which is a function of time *t*, can be defined as:

$$Nu(t) = \frac{1}{\overline{h}(t)} \sqrt{\frac{\sum_{i=1}^{N_c} \left(h_i(t) - \overline{h}(t)\right)^2}{N_c}} \tag{14}$$

Venkatesh [9] performed research on polishing glass moulds and proposed a reference for real data on non-uniformity, shown in Fig. 11, by using the polishing time versus surface roughness curves, which indicated that initial rapid improvement of roughness followed by a leveling off, manifesting a saturation effect. They also found the familiar knee curve, after which an increase in polishing time does not improve the surface finish.

4 Results and comparison

In the pad dressing process, the polishing pad is subjected to a dressing force. A number of typical deformed shapes of the polishing pad along the radial direction subjected to different dressing forces are shown in Fig. 12, which reveals that the deformation in the center of the dresser is obvious, and similar deformed-shapes are obtained for different dressing forces.

A number of simulations were carried out to investigate the relationship between the non-uniformity and machining parameters. Time step *dt* was set to 0.01 s in this study. Figures 13, 14, 15 show the histories of abrasive depth $\overline{h}$ with dressing time, different angular speeds of the holder ω_d and different translation speeds of the holder V_d, respectively.

Figure 13 shows that $\overline{h}$ becomes large when the dressing force increases. This is because the large dressing force *fc* causes the pad to deform severely, causing a higher plastic zone. Figure 14 shows that $\overline{h}$ is similar for different angular speeds of the dresser, except for the rpm near the angular speeds of the pad (20 rpm). From Fig. 15, $\overline{h}$ is also similar for different translation speeds of the holder, except for the speed of about 3 mm per second. Moreover, a model to

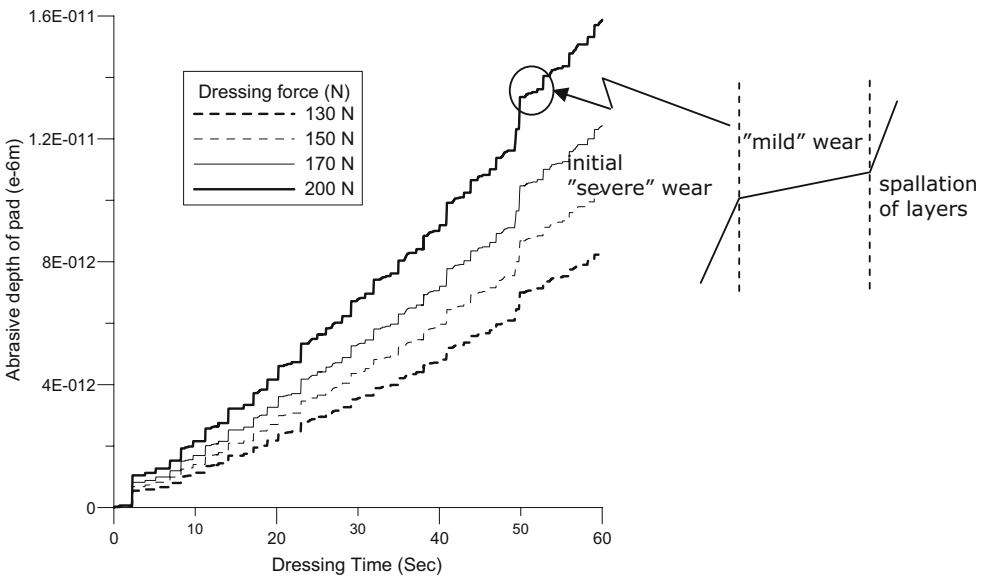

Fig. 13 Abrasive depth $\overline{h}$ histories for the planarization process with different dressing forces f_c (E=139.47 Mpa, ν=0.3, d_n=200 No./cm^2, ω_d=14 rpm, ω_p=20 rpm, V_d=3 mm/s, r_g=0.01 mm, N_d=8, r_d=10 mm, r_c=50 mm, r_p=400 mm, H= 4 mm, e=200 mm, and c=0.5)

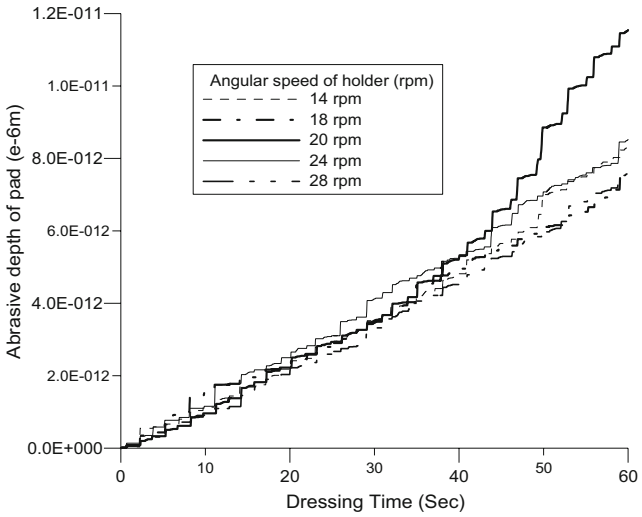

Fig. 14 Abrasive depth $\overline{h}$ histories for the planarization process with dressing time (f_c=130 N, E=139.47 Mpa, ν=0.3, d_n=200 No./cm^2, ω_p=20 rpm, V_d=3 mm/s, r_g=0.01 mm, N_d=8, r_d=10 mm, r_c=50 mm, r_p=400 mm, H=4 mm, e=200 mm, and c=0.5)

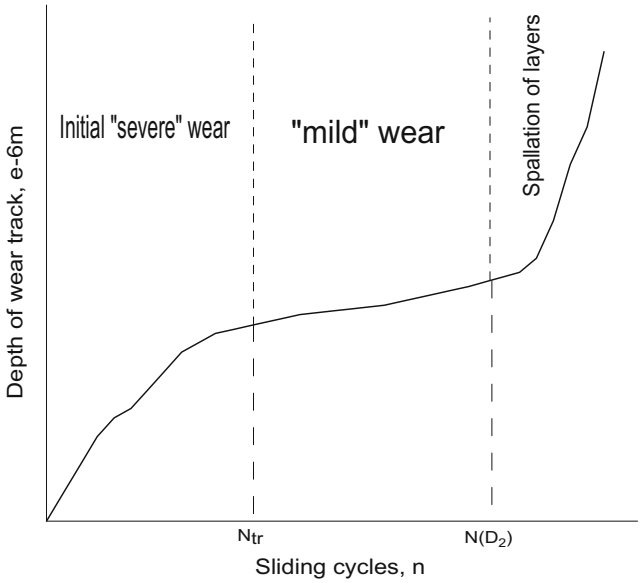

Fig. 16 A schematic diagram showing the variation of wear depth of the coating as a function of number of contact cycles of the disk (coating surface) with the ball, as predicted by the wear model [12]

calculate the depth of the wear track conducted by Jiang [12], as shown in Fig. 16, is introduced to investigate the validity of simulation results of abrasive depth. Jiang investigated the tribological behavior of the composite coatings under various conditions in a continuous ball-on-disk sliding wear machine in dry air. Figure 16 shows that the wear model of depth of wear track comprises of three stages: initial severe wear, mild wear, and spoliation of layers. From simulation results of abrasive depth, shown in Fig. 13, the three stages also exist in the processing histories in a short period of time. Therefore, the model to calculate abrasive depth can be an acceptable estimation.

Figures 17, 18, 19 show the histories of non-uniformity Nu with dressing time, different angular speeds of holder ω_d and different translation speeds of the holder, V_d, respectively. These figures indicate an initial rapid improvement followed by a leveling off, manifesting a saturation effect.

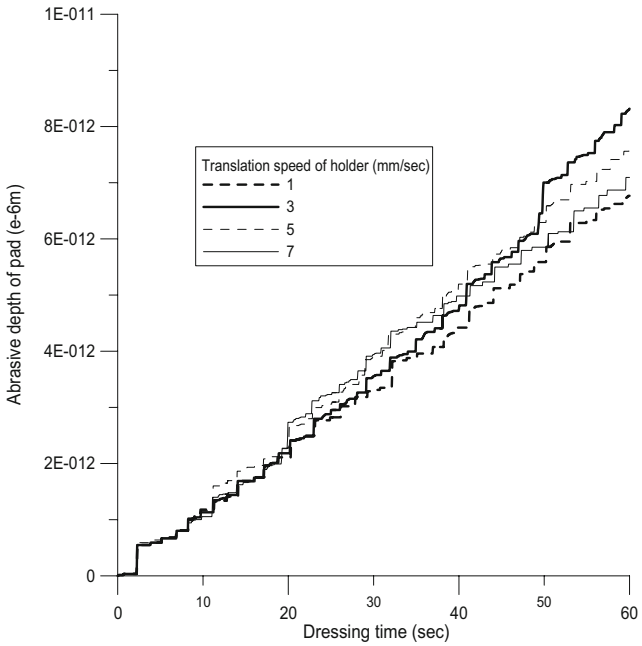

Fig. 15 Abrasive depth ($\overline{h}$) histories for the planarization process with dressing time (f_c=130 N, E=139.47 Mpa, ν=0.3, d_n=200 No./cm^2, ω_d=14 rpm, ω_p=20 rpm, r_g=0.01 mm, N_d=8, r_d=10 mm, r_c=50 mm, r_p=400 mm, H=4 mm, e=200 mm, and c=0.5)

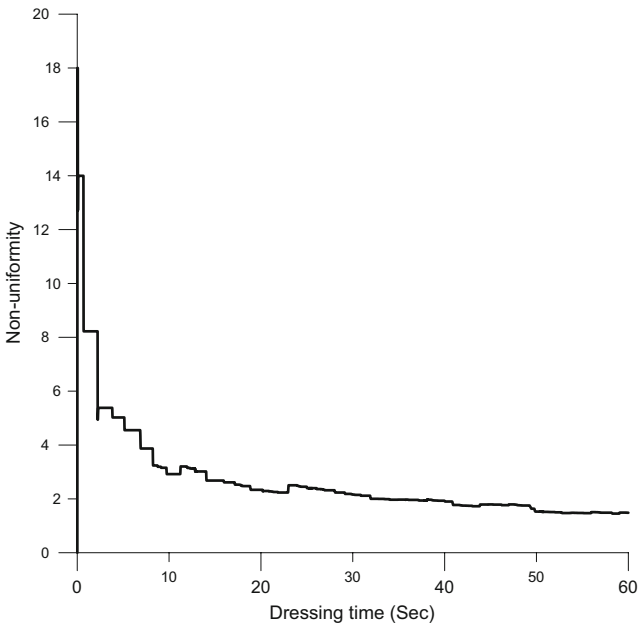

Fig. 17 Non-uniformity (Nu) histories for the planarization process (f_c=130 N, E=139.47 Mpa, ν=0.3, d_n=200 No./cm^2, ω_d=14 rpm, ω_p=20 rpm, V_d=3 mm/s, r_g=0.01 mm, N_d=8, r_d=10 mm, r_c=50 mm, r_p=400 mm, H=4 mm, e=200 mm, and c=0.5)

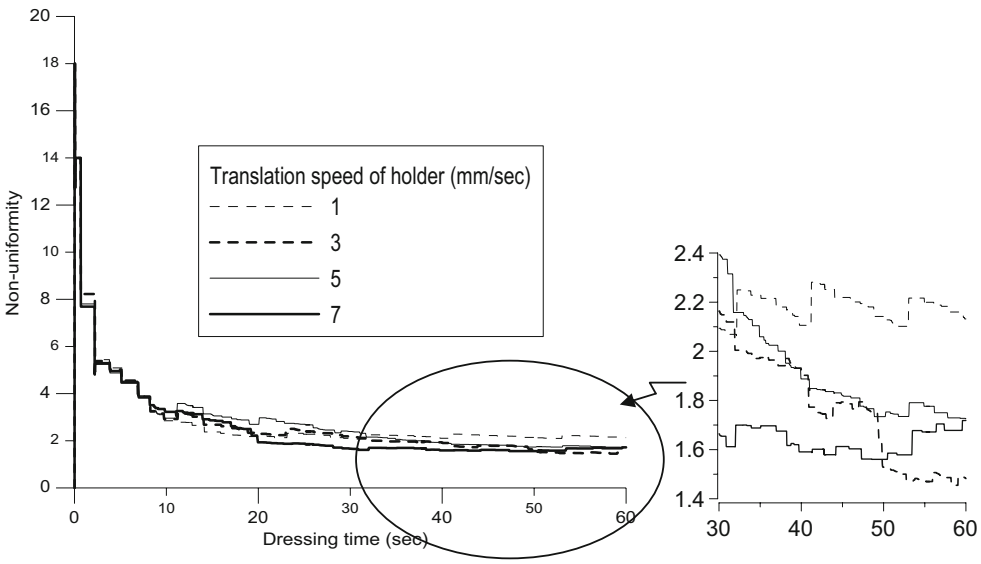

Fig. 18 Non-uniformity (*Nu*) histories for the planarization process with different translation speeds of the holder V_d (f_c= 130 *N*, *E*=139.47 Mpa, ν=0.3, d_n=200 No./cm^2, ω_d=14 rpm, ω_p=20 rpm, r_g=0.01 mm, N_d= 8, r_d=10 mm, r_c=50 mm, r_p= 400 mm, *H*=4 mm, *e*=200 mm, and *c*=0.5)

Figure 17 indicates that *Nu* is substantially uniform, becoming a horizontal line after a certain dressing time. In this paper, the purpose of the planarization process is to refresh the pad by polishing the surface of the pad. Therefore, the non-uniformity *Nu(t)*=0 at *t*=0, but is increased abruptly at the beginning of planarization process. Then, the non-uniformity has a rapid initial improvement followed by a leveling off, manifesting a saturation effect. This figure shows the *Nu* limitation for the planarization process. Figure 18 shows that *Nu* is also similar for different translation speeds of the holder, and Fig. 19 shows that *Nu* is similar for all different angular speeds of the dresser, except for the rpm near the angular the speed of the pad (20 rpm).

A higher dressing force with a dresser speed near the pad speed, and a moderate translation speed seemed to be the optimal machining parameters for the pad planarization process. In other words, the goal of increasing material removal corresponding with lower non-uniformity dressing is valid by using these data in the pad planarization. The reasons are that the maximum relative speed between the pad and the dresser occur when the dresser speed is close to the pad speed and it has a moderate translation speed, resulting in lower non-uniformity. Moreover, significant deformation of the pad occurs under a higher dressing force, resulting in the increasing of the material removal rate.

5 Conclusion

A model to estimate non-uniformity was explored in this paper and compared with experimental data collected by

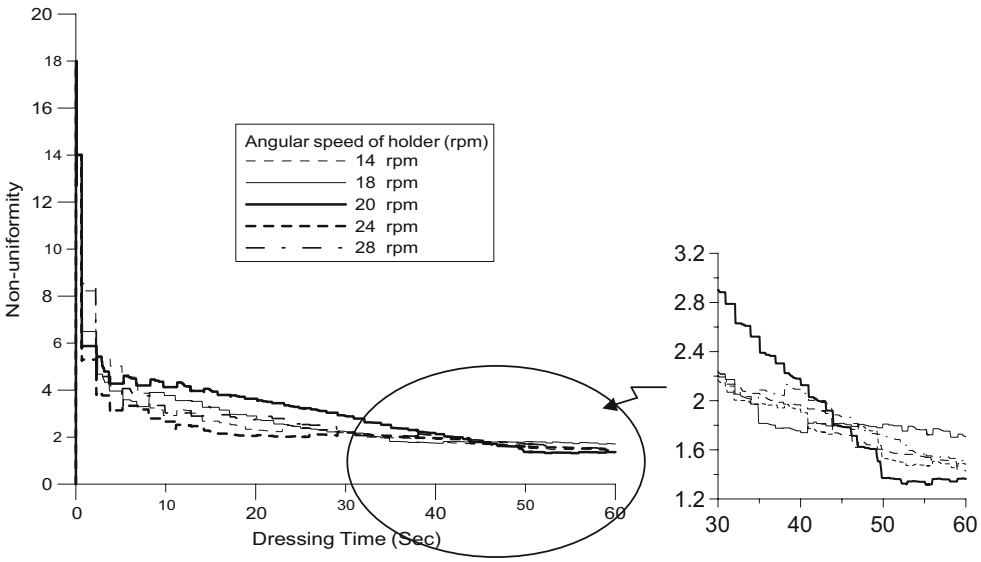

Fig. 19 Non-uniformity (*Nu*) histories for the planarization process with different angular speeds of the holder ω_d (f_c= 130 *N*, *E*=139.47 Mpa, ν=0.3, d_n=200 No./cm^2, ω_p=20 rpm, r_g=0.01 mm, N_d=8, r_d=10 mm, r_c=50 mm, r_p=400 mm, *H*= 4 mm, *e*=200 mm, and *c*=0.5)

Goryacheva and Venkatesh. The model is a good simulation of non-uniformity for the pad dressing in the planarization process. Moreover, a simulation of the planarization process was undertaken using various machining parameters consisting of abrasive forces, rotational speed of the dresser, and various machining paths. In conclusion, the results of this model reveal that in processing planarization, a higher dressing force with the dresser at a speed close to the pad speed, and a moderate translation speed increase the material removal rate corresponding with lower non-uniformity dressing.

Acknowledgements This study was support by the National Science Council, Republic of China under contract numbers: NSC-93-2212-E-168-018 and NSC-95-2622-E-168-015-CC3.

References

1. Lin SC, Wu ML (2002) A study of the effects of polishing parameters on material removal rate and non-uniformity. Int J Mach Tools Manuf 42(1):99–103
2. Preston FW (1927) The theory and design of plate glass polishing machine. J Soc Glass Technol 214–256
3. Zhou YY, Davis EC (1999) Variation of polishing pad shape during pad dressing. Math Sci Eng B68(2):91–98
4. Tseng WT, Liu CW, Dai BT, Yeh CF (1996) Effects of mechanical characteristics on the chemical-mechanical polishing of dielectric thin films. Thin Solid Films 290–291:458–463
5. Xie Y, Bhushan B (1996) Effects of particle size, polishing pad and contact pressure in free abrasive polishing. Wear 200(1–2):281–295
6. Goryacheva IG (1998) Contact mechanics in tribology. Kluwer, Boston
7. Horng TL (2003) An analysis of the pad deformation for improved planarization. Key Eng Mater 238–239:241–246
8. Thomas FA, Dennis S, Kevin M (1997) Cartesian coordinate maps for chemical mechanical planarization uniformity characterization. Thin Solid Films 308–309:512–517
9. Venkatesh VC, Zhaowei Z, Erning W (1996) Studies on polishing of glass moulds after lapping with hard and soft pellets. J Mater Process Technol 62(4):415–420
10. Chen CC, Juang YS, Lin WZ (2002) Generation of fractal toolpaths for irregular shapes of surface finishing areas. J Mater Process Technol 127(2):146–150
11. Dowson D, Higginson GR (1963) Theory of Roller Bearing Lubrication and Deformation. Proc. Lubrication and Wear Convention, Instn. Mech. Engrs., London, Paper 19:216–227
12. Jiang J, Arnell RD, Tong J (1998) An investigation into the tribological behaviour of DLC coatings deposited on sintered ferrous alloy substrate. Wear 214(1):14–22